Effect of Polydispersity on the Formation of Vesicles from Amphiphilic Diblock Copolymers

Ying Jiang,[†,‡] Tao Chen,[†,‡] Fangwei Ye,[‡] Haojun Liang,[*,†,‡] and An-Chang Shi[*,§]

Hefei National Laboratory for Physical Sciences at Microscale, University of Science and Technology of China, Hefei, Anhui 230026, People's Republic of China; Department of Polymer Science and Engineering and Department of Physics, University of Science and Technology of China, Hefei, Anhui 230026, People's Republic of China; and Department of Physics and Astronomy, McMaster University, Hamilton, Ontario L8S4M1, Canada

Received February 28, 2005; Revised Manuscript Received April 24, 2005

ABSTRACT: Using a continuous chain length distribution, the effect of polydispersity on the structures of vesicles self-assembled by amphiphilic polydisperse diblock copolymers in dilute solutions is investigated by two-dimensional (2D) real-space self-consistent-field theory. It is discovered that larger polydispersity favors the formation of smaller vesicles or quasi-vesicles. This polydispersity effect can be attributed to the segregation of copolymers according to their chain lengths. Two types of chain segregations are observed. First of all, the shorter chains tend to localize at the A/B interfaces while the longer chains tend to stretch to the outer surfaces. Second, there is a separation of copolymers to the inner and outer monolayers of the bilayers, leading to a longer average chain length in outer monolayer.

1. Introduction

Block copolymers are formed by chemically linking different polymer chains together. Because of the repulsive interactions between different blocks and the topological constraint that the subchains are linked permanently, block copolymers self-assemble to form a variety of ordered structures in melts and concentrated solutions.[1] In dilute solutions, it is well-known that amphiphilic block copolymers form micelles above the critical micelle concentration.[2] Besides the usual spherical micelles, previous studies have demonstrated that amphiphilic block copolymers are able to self-assemble into various complex microstructures in dilute solution. Among the many observed complex microstructures, polymeric vesicles formed from diblock copolymer bilayers have been the focus of active studies in recent years.[3−8] This is partly due to the biological significance of vesicles. It has been suggested that this cell-like structure possesses the potential of application in drug delivery systems and artificial cells.[9]

Because of their importance, a variety of theoretical approaches, including coarse-grained surface models,[10−12] Brownian dynamic simulations,[13,14] Monte Carlo simulations,[15,16] and dissipative particle dynamics,[17] have been used to investigate the formation of vesicles. In addition to these theoretical approaches, the self-consistent-field theory (SCFT), which has been very successful for the study of the ordered phases of block copolymers, provides a powerful tool for the study of vesicles. SCFT is a coarse-grained field theoretical technique in which the polymer densities are the primary variables. The theory has its origin from the field theoretical approach of Edwards in the 1960s.[18] Helfand and others explicitly adopted the theory to treat self-assembly of block copolymers.[19] In recent years SCFT has become a powerful tool to study the self-assembly of block copolymers.[20−24] For the bulk ordered phases, Matsen and Schick have successfully solved the SCFT equations numerically, using a restricted Fourier basis which were selected on the basis of the assumed morphological symmetries.[20] The Matsen−Schick approach is efficient, and it allows accurate calculations of the free energies, which are used to construct phase diagrams for the block copolymer systems. However, for the exploratory research on the more complex copolymer systems of higher degree of architectural complexity, this reciprocal space approach is not applicable since it requires that the symmetry of the ordered structures to be known a priori. A possible method to circumvent this problem is to solve the SCFT equations in real space. In particular, Drolet and Fredrickson suggested an implementation where low free energy morphologies are found by relaxation from random potential fields.[22] A similar real-space approach has also been suggested by Bohbot-Raviv and Wang.[25] It is noticed that solving the SCFT equations in three dimension presents a computationally challenging task and must of the previous work were carried out in two dimensions.

Although SCFT has been very successful for studying bulk ordered phases, the application of SCFT to the more challenging problem of self-assembled complex structures in dilute copolymer solutions is still in its infancy. This is largely due to the difficulty of searching for the many metastable states which are intrinsic in the system. For the study of the complex micelle structures, a priori knowledge about the morphology is not available. Therefore, real-space approaches, such as the one suggested by Drolet and Fredrickson, become the method of choice. Recently, Liang and co-workers have successfully performed two-dimensional (2D) space real-space SCFT studies on the formation of complex micelles (e.g., circlelike and linelike micelles corresponding to spherelike and rodlike micelles in 3D or

[†] Hefei National Laboratory for Physical Sciences at Microscale, UST China.
[‡] Department of Polymer Science and Engineering and Department of Physics, UST China.
[§] McMaster University.
* To whom all correspondence should be addressed: e-mail hjliang@ustc.edu.cn, shi@mcmaster.ca.

10.1021/ma050424j CCC: $30.25
Published on Web 06/25/2005

vesicles) of amphiphilic diblock copolymers in dilute solution.[26] This encouraging initial study demonstrated the potential of SCFT for the study of complex micelle structures.

In most of the theoretical approaches, it is assumed that the polymers are monodisperse. However, most, if not all, of the synthetic polymers are polydisperse. It is well-known that many of the unique static and dynamic properties of polymers depend on chain length,[27,28] and it is expected that larger polydispersity will influence those properties. For example, polydispersity effects on relaxation of concentration fluctuations in diblock melts and solutions have been investigated.[29] There have been a few theoretical studies incorporating polydispersity into block copolymer models. However, most of these studies are restricted to weak/strong segregation limits[30−32] or SCFT models[33,34] that mimic polydispersity using binary mixtures of block copolymers with different lengths. Recently, Sides and Fredrickson have proposed an efficient SCFT method to study the effect of polydispersity on the bulk phase behavior of block copolymer melts.[35,36]

In this paper we study the self-assembly of dilute polydisperse AB diblock copolymer solutions using a 2D real-space SCFT approach. Our theoretical framework is an extension of the SCFT for a polydisperse melt developed by Sides and Fredrickson.[35,36] In principle, both blocks of the copolymer can be polydisperse with different molecular weight distributions. In this first study of the system, we focus on a simpler model of amphiphilic AB diblock copolymers. In the model only one of the two blocks is assumed to be polydisperse, while the other block is assumed to be monodisperse. The polydispersity is characterized by a continuous molecular weight distribution. In the model, the polydisperse block can be either the hydrophilic one or the hydrophobic one. It should be noted that the results from the study of this simple model are relevant to block copolymers produced by the new controlled free radical polymerization methods which are often much more "controlled" for one type of monomer than another. In what follows we will demonstrate that our studies are useful for understanding the mechanism for the effect of polydisperse hydrophilic or hydrophobic blocks on the formation of the vesicle in 2D.

2. Theoretical Framework

The polymers are modeled as flexible Gaussian chains. In the model system, polydisperse amphiphilic diblock copolymers with segments A, B, and solvent molecules S are included in a volume V. The volume fractions of segments A and B in the system are specified by f_A and f_B, respectively. The copolymer volume fraction is $f_P = f_A + f_B$. As a result of the incompressibility condition, the volume fraction of the solvent is $f_S = 1 - f_P$. In the SCFT approach, the statistics of a single copolymer chain is modeled by a Gaussian chain in a set of effective chemical potential fields ω_I, where the subscript I represents block species A or B, respectively. The chemical potential field ω_I, which represents the monomer−monomer interactions between different components within the mean-field approximation, is conjugate to the segment density field, ϕ_I, of block species I. Similarly, solvent molecules are considered to be in an effective chemical potential field ω_S that is conjugate to the solvent density field ϕ_S. In terms of these variables, the free energy density (in unit of k_BT) of the system is specified by

$$F = -f_S \ln(Q_S/V) - \frac{f_P}{N_n}\sum_0^\infty dN'\, \Psi(N') \ln(Q_P/V) + \frac{1}{V}\int dr\, [\chi_{AB}N_n\phi_A\phi_B + \chi_{SA}N_n\phi_A\phi_S + \chi_{BS}N_n\phi_B\phi_S - \omega_A\phi_A - \omega_B\phi_B - \omega_S\phi_S - P(1 - \phi_A - \phi_B - \phi_S)] \quad (1)$$

where N_n is the number-average chain length, χ_{ij} is the Flory−Huggins interaction parameter between species i and j, and P is a Lagrange multiplier (as a pressure) which ensures the incompressibility condition. The single molecular partition function of the solvent in the effective chemical potential field ω_S is defined by $Q_S = \int dr \exp(-\omega_S/N_n)$. The partition function of a single chain $Q_P = \int dr\, q(r,N'/N_n)$ is an explicit function of N' and is weighted by $\Psi(N')$. Here $\Psi(N')$ is the normalized probability density for chain length. The end-segment distribution function $q(r,s)$ gives the probability of the section of a chain, with contour length s and containing a free chain end, has its "connected end" located at r. The parametrization is chosen such that the contour variable s increases continuously from 0 to N'/N_n, where N' represents the total length of a particular chain corresponding from one end of the chain to the other. Using a flexible Gaussian chain model of the single-chain statistics, the function $q(r,s)$ satisfies the following modified diffusion equation

$$\frac{\partial}{\partial s}q(r,s) = \begin{cases} R_{g0}^2\nabla^2 q(r,s) - \omega_A q(r,s) & 0 < s < N_A/N_n \\ R_{g0}^2\nabla^2 q(r,s) - \omega_B q(r,s) & N_A/N_n < s < N'/N_n \end{cases} \quad (2)$$

where the lengths are scaled by R_{g0}, the (overall) radius of the gyration of an unperturbed chain. The appropriate initial condition is $q(r,0) = 1$. Similarly, a second distribution function $q'(r,s)$ (containing the other chain end) is also a solution of eq 2 with the initial condition $q'(r,N') = 1$.

The mean-field SCFT equations are obtained by the saddle point approximation, where one sets $\delta F/\delta\phi_i = \delta F/\delta P = \delta F/\delta\omega_i = 0$, leading to the following set of equations:

$$\omega_A(r) = \chi_{AB}N_n(\phi_B(r) - f_B) + \chi_{SA}N_n(\phi_S(r) - f_S) + P(r) \quad (3)$$

$$\omega_B(r) = \chi_{AB}N_n(\phi_A(r) - f_A) + \chi_{BS}N_n(\phi_S(r) - f_S) + P(r) \quad (4)$$

$$\omega_S(r) = \chi_{SA}N_n(\phi_A(r) - f_A) + \chi_{BS}N_n(\phi_B(r) - f_B) + P(r) \quad (5)$$

$$\phi_A(r) + \phi_B(r) + \phi_S(r) = 1 \quad (6)$$

$$\phi_A(r) = \int_0^\infty dN' \frac{\Psi(N')}{Q_P(N'/N_n)}\int_0^{N_A/N_n} ds\, q(r,s)\, q'(r,1-s) \quad (7)$$

$$\phi_B(r) = \int_0^\infty dN' \frac{\Psi(N')}{Q_P(N'/N_n)} \int_{N_A/N_n}^{N'/N_n} ds\, q(r,s)\, q'(r,1-s) \tag{8}$$

$$\phi_S(r) = \frac{\exp(-\omega_S(r)/N_n)}{Q_S} \tag{9}$$

Here, constant shifts in the potential are introduced in the eqs 3−5. Similar to ref 36, an AB diblock copolymer is assumed to have an A block with fixed chain-length N_A and a B block with variable chain lengths. A continuous molecular weight distribution function, the Schulz chain length distribution[37]

$$\Psi(N) = \begin{cases} 0 & N < N_A \\ [(N-N_A)/N_b]^{\alpha-1} \dfrac{\exp[-(N-N_A)/N_b]}{N_b \Gamma(\alpha)} & N \geq N_A \end{cases} \tag{10}$$

is chosen as a model of the polydisperse AB blocks with overall number-average $N_n = \alpha N_b + N_A$. The parameter α is related to the polydispersity index of the B block, $I^B_{pdi} = (\alpha + 1)/\alpha$. Similarly, for the cases in which the A block has variable chain lengths and B block has a fixed chain length, the formula (10) will be modified accordingly.

The mean-field SCFT equations (eqs 3−9) are solved directly in real space by using a combinatorial screening algorithm proposed by Drolet and Fredrickson.[22] The essence of the method is to search for low free energy solutions of the SCFT equations starting from different initial conditions. As a first step of the study, the calculations are restricted to two dimensions. Furthermore, periodic boundary conditions are used in the calculations. The initial values of the fields ω are constructed using the relation $\omega_j(r) = \Sigma_{i\neq j}\chi_{ij}(\phi_i(r) - f_i)$, where f_i represents the average volume fraction of the copolymer segments or solvent and $\phi_i(r) - f_i$ satisfies Gaussian distributions:

$$\langle(\phi_i(r) - f_i)\rangle = 0$$

$$\langle(\phi_i(r) - f_i)(\phi_j(r') - f_j)\rangle = \beta f_i f_j \delta_{ij}\delta(r - r') \tag{11}$$

Here, the parameter β characterizes the intensity of the density fluctuations at the initial temperature. Using a "pseudospectral method",[38,39] the modified diffusion equations are solved to obtain the end-integrated propagators, $q(r,s)$ and $q'(r,s)$. Next, the density field ϕ_I of species I, conjugate to the chemical potential field ω_I, can be evaluated based on eqs 7−9. For eqs 7 and 8, the n_g-point Gaussian quadrature scheme[36,40] is adopted (e.g., $n_g = 4-8$ is sufficient for the results presented). To enforce the incompressibility of the system, the effective pressure field, $P = C_2C_3(\omega_A + \omega_B) + C_1C_3(\omega_B + \omega_S) + C_1C_2(\omega_A + \omega_S)/2(C_1C_2 + C_2C_3 + C_1C_3)$, is obtained through solving eqs 3−6, where $C_1 = \chi_{SA} + \chi_{BS} - \chi_{AB}$, $C_2 = \chi_{SA} + \chi_{AB} - \chi_{BS}$, and $C_3 = \chi_{AB} + \chi_{BS} - \chi_{SA}$. The chemical potential field ω_I can be updated by using the equation $\omega_I^{new} = \omega_I^{old} + \Delta t(\delta F/\delta\phi_I)^*$, where $(\delta F/\delta\phi_I)^* = \sum_{M\neq I}\chi_{IM}(\phi_M(r) - f_M) + P(r) - \omega_I^{old}$ acts as a chemical potential force and the time step is set at $\Delta t = 0.1$. The above steps are iterated until the free energy converges to a local minimum, where the self-assembled structure corresponds to a metastable state. This iteration scheme represents a pseudodynamical process which follows the steepest descent paths on the free energy landscape to the nearest metastable state. We note that this algorithm does not correspond to real dynamics of the ordering processes. It is simply a method to evolve a system as rapidly as possible to a free energy minimum satisfying some certain constraints, e.g., incompressibility. It has been demonstrated that, starting from different the initial conditions, various metastable states can be reached.[26] Therefore, the iteration method presented above provides an efficient combinatorial technique to search for different self-assembled micelle structures.

The numerical simulations were carried out in a 2D space represented by an $L \times L$ box, which is divided into a 128×128 lattice. The size of the box L is chosen to ensure that the simulation box is larger than the size of the vesicle. For most of the calculations the box size is taken as $L = 32$ and grid size is $\Delta x = 0.25$, where all lengths are measured in unit of R_{g0} (unperturbed mean-square radius-of-gyration of a copolymer chain). The simulation for each sample was carried out until the phase pattern was stable and invariable with time, and the free energy change is negligible, $\Delta F < 10^{-6}$. Starting from a homogeneous block copolymer solution, the simulation was repeated for 10 to ~20 times using different initial random states and different random numbers to ensure that the observed phenomena are not accidental.

3. Results and Discussion

In most of the calculations, the diblock copolymer chains are assumed to have an average chain length $N_n = 30$ and an average hydrophilic block volume fraction of 0.1333, corresponding to a crew-cut-type diblock copolymer. The volume fraction of polymers in the solution is kept at $f_P = 0.1$ to ensure the system to be a dilute solution. The interaction parameters are assumed to have the following values, $\chi_{AB}N_n = 24.0$, $\chi_{AS}N_n = -9.0$, and $\chi_{BS}N_n = 30.0$; therefore, the A-block is hydrophilic. In addition, to compare the results at different polydispersity index I^K_{pdi} of block K (K can be either the A or B block), the Schulz parameter N_k is adjusted such that the average monomer densities and $\chi_{ij}N_n$ are constant. Similar to ref 26, our simulation shows that a small initial density fluctuation amplitude on the order of $\beta = 10^{-6}$, corresponding to a longer correlation length, results in the formation of vesicles. The SCFT studies reported below were carried out for two cases, corresponding to a polydisperse hydrophilic block (A) and a polydisperse hydrophobic block (B).

3.1. Polydisperse Hydrophilic Blocks. In this subsection the effect of hydrophilic block polydispersity is investigated. The computations were carried out for diblock copolymers with a polydisperse hydrophilic block and a monodisperse hydrophobic block. The observed vesicle-like microstructures corresponding to different polydispersity indexes I^A_{pdi} of the hydrophilic blocks are shown in Figure 1. These results demonstrate that the microstructures assembled in dilute diblock copolymer solutions depend sensitively on the polydispersity, showing vesicles (Figure 1a), mixture of vesicles and quasi-vesicle (Figure 1b) [details about the structures of the quasi-vesicle will be given in the following section], pure quasi-vesicle (Figure 1c), and circlelike (corresponding to cylindrical in 3D) micelles (Figure 1d) in 2D, as the polydispersity index of hydrophilic blocks is increased. To obtain detailed information about these

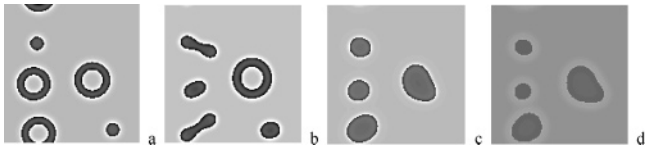

Figure 1. Self-assembled structures of amphiphilic diblock copolymers with polydisperse A (hydrophilic) blocks of different polydispersity index I^{A}_{pdi}. The patterns are obtained from the same value of initial density fluctuation β (equals to 10^{-6}) with the parameters $\chi_{AB}N_n = 24.0$, $\chi_{AS}N_n = -9.0$, $\chi_{BS}N_n = 30.0$, $n_g = 6$. (a) $I^{A}_{pdi} = 1$ (monodisperse); (b) $I^{A}_{pdi} = 1.4$; (c) $I^{A}_{pdi} = 2.0$; (d) $I^{A}_{pdi} = 3.5$. The gray and white areas present the hydrophobic and hydrophilic segments, respectively.

microstructures, the density distributions of the hydrophilic and hydrophobic components as well as the solvents are analyzed. For the case of monodisperse system corresponding to Figure 1a, the density profiles (not shown here since they are exactly the same as the ones reported in ref 26) have a bimodal feature; i.e., both the solvent and the hydrophilic components fully occupy the center of the vesicle while the hydrophobic blocks form the "wall" of the vesicle. The basic building unit is the bilayer, which is composed of two monolayers, or an inner leaf and an outer leaf. The hydrophilic blocks in the outside shield the unfavorable repulsive interactions between the solvents and hydrophobic segments. For the monodisperse case (Figure 1a), the two leaves of the bilayers are composed of exactly the same diblock copolymers. However, for the cases of polydisperse diblock copolymers, it is possible that the block copolymers with different molecular weights segregate to the inner and outer leaves, so that the stretching energy of the polymers can be minimized. In other words, it is possible that the block copolymers in the inner and outer leaf have different molecular weight distribution. This segregation of polymers with different chain length can be analyzed by examining the density contributions from the different Gaussian quadratures parametrized by n_g (=6). It should be noted that in the Gaussian quadrature scheme larger values of g correspond to chains with higher molecular weight, i.e., longer chains. Therefore, each of the n_g terms may be interpreted as the contribution to the overall density from the chains with different length. In Figure 2 the individual density contributions from each n_g are plotted for the case of a polydispersity index $I^{A}_{pdi} = 1.4$. From a cross-section through a vesicle domain, the density profiles of the polymers (Figure 2a) exhibit the typical characteristics of vesicles with bimodal feature of the hydrophobic components. On the other hand, the density contributions from different Gaussian quadratures (Figure 2b,c) clearly indicate that the copolymers are segregated according to the chain length. For the hydrophilic blocks, a semiquantitative analysis of this separation can be performed by approximating the peak values in the density profiles as the dominant density distribution for different chain lengths. In Figure 2b, the dotted lines denoted by "C" and "W" identify the center of the vesicle and the center of the bilayer, respectively. The A block density contributions from different n_g terms are distributed on the inside surface [inner leaf] and outside surface [outer leaf] of the bilayer. To proceed, we introduce two parameters, r_g^{in} and r_g^{out} (marked in Figure 2b), defined as the distances from the peaks of the density distributions of the hydrophilic segments A in the inner and outer leaf. From Figure 2b, we observe

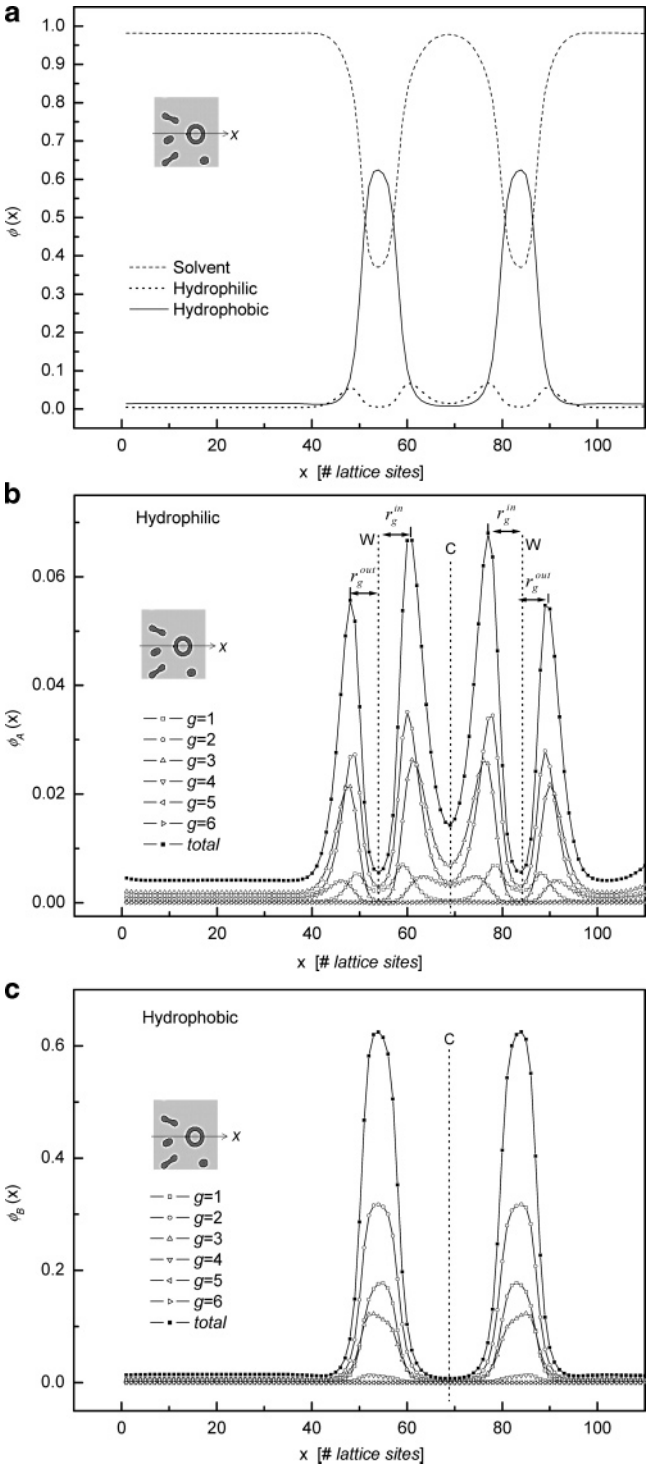

Figure 2. Density distribution of a vesicle for a diblock copolymer with polydisperse A (hydrophilic) blocks for $I^{A}_{pdi} = 1.4$ and $n_g = 6$. The inset shows two-dimensional density configurations corresponding to Figure 1b. (a) Density contributions from A (hydrophilic) segments, B (hydrophobic) segments, and S (solvent); (b, c) Contributions from each of the n_g terms. In (b) and (c), the dotted line with C and W denotes the center of a large vesicle and the center of the wall in a large vesicle, respectively. r_g^{in} and r_g^{out} represent the distance from the peak of total density distribution of the hydrophilic segments A located at inside or outside of the wall to the center of the wall of the vesicle. Note that (a), (b), and (c) have different scales.

that, if $g_2 > g_1$, then we have $r_{g2}^{in(out)} > r_{g1}^{in(out)}$, indicating that, in comparison with the longer hydrophilic segments, the shorter ones tend to localize at the A−B

interfaces. This segregation of block according to chain length has been observed by Sides and Fredrickson for the bulk phases of polydisperse diblock copolymer melts.[36] Furthermore, there is another segregation of the copolymers between the inner and outer leaves, as shown in Figure 2c. For smaller values of $g = 1$ and $g = 2$, the density distributions of the B-block are more or less symmetric, indicating that there is no separation between the inner and outer monolayers for short chains. However, for larger values of $g > 3$, the density profiles show a clear asymmetric distribution, indicating that there are more longer blocks in the outer monolayer. It can be concluded that there is a separation of the diblock copolymers into the two leaves according to the chain lengths. It is noted that the contributions from $g = 5$ and 6 in Figure 2b,c are negligible, indicating that $n_g = 4$ gives sufficiently accurate results for the system. In summary, we can understand the structure of the large vesicle influenced by hydrophilic polydispersity as follows. The basic structure of the bilayer is composed of two leaves of monolayers with the hydrophilic blocks in contact with the solvents. This is similar to the bilayer structure from monodisperse diblock copolymers. The polydispersity of the hydrophilic block leads to two changes in the distribution of the polymers. First of all, the short chains tend to be located close to the hydrophilic−hydrophobic interfaces. This segregation of polydisperse blocks is also observed in the bulks phases studied by Sides and Fredrickson.[36] Second, there is a segregation of the polymers between the inner and outer monolayers (leaves), leading to a slight difference in the block length distributions for the polymers located in these two leaves. The shorter hydrophilic blocks in the inner leaf lead to a change of the spontaneous curvature of the bilayers, favoring smaller vesicles.

For larger hydrophilic polydispersity index I^{A}_{pdi}, large vesicles are no longer observed in our simulations, and instead, the structures shown in Figure 1c are typically observed. Taking one of the structures from Figure 1c, the density distributions of the A, B segments and the solvent (S) are shown in Figure 3. The first impression one would get by inspecting the structures in Figure 1c was that they are similar to the usual micelles. However, a detailed analysis reveals that these structures possess some characteristics of the vesicles. In particular, the density distribution of the hydrophobic segments has a quasi-bimodal feature similar to vesicles (see Figure 3a). From the density profile of the hydrophobic blocks, the solvent concentration in the center of the structure is about 45%. For this reason we term these structures as quasi-vesicles in order to distinguish them from the large vesicle observed for systems with a smaller polydisperse index as well as the usual micelles.

To distinguish the contribution from the chains with long or short hydrophilic block, the density distributions of hydrophilic segments of chains with different hydrophilic block length are shown in Figure 3b. From the density distributions of different chain lengths, we can conclude that the hydrophilic blocks behavior varies according to their lengths. In the corona region, the shorter blocks are localized at the interfaces, while the longer blocks are extended to form a brush. Inside the structure, on the other hand, the shorter hydrophilic blocks are extended into the center of the micelle, while the longer hydrophilic blocks are excluded from the interior of the micelle. Therefore, there is a strong separation of the block copolymers according to the

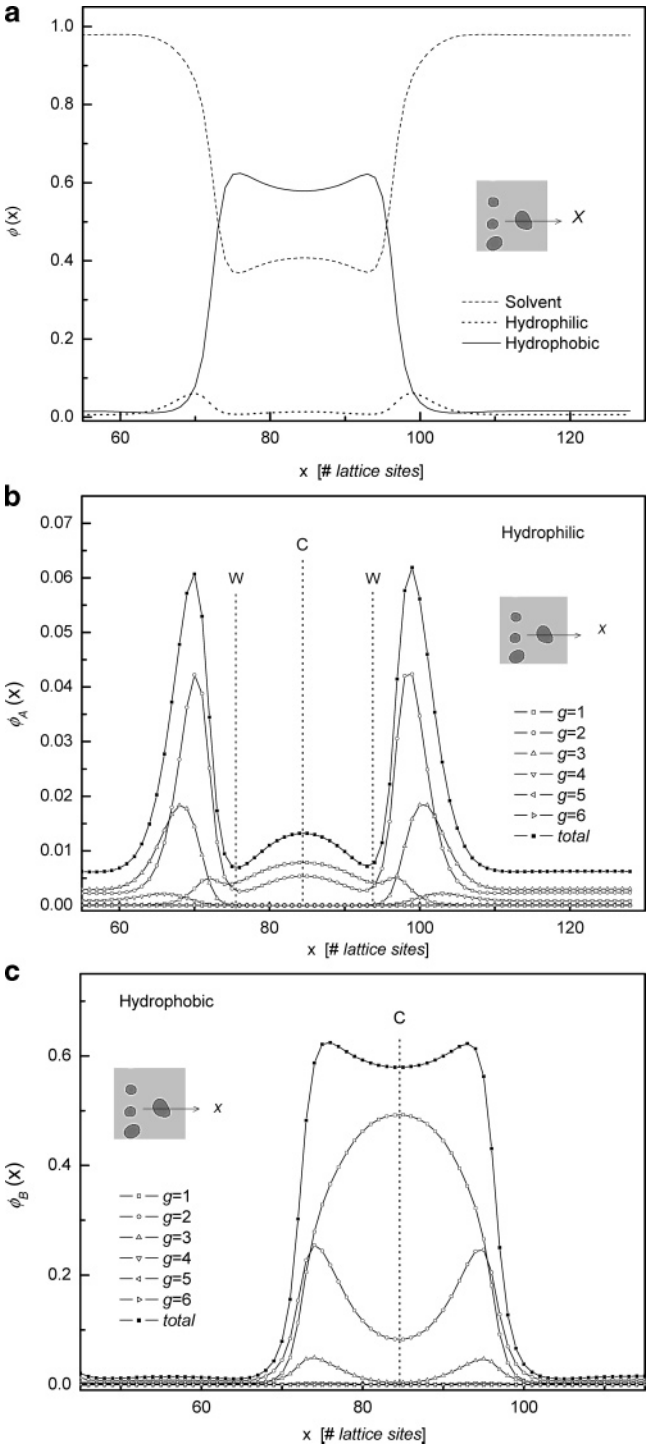

Figure 3. Density distribution of the quasi-vesicle for polydisperse A (hydrophilic) blocks with $I^{A}_{pdi} = 2.0$ and $n_g = 6$. The inset shows two-dimensional density configurations corresponding to Figure 1c. (a) Density contributions from A (hydrophilic) segments, B (hydrophobic) segments, and S (solvent). (b, c) Contributions from each of the n_g terms. In (b) and (c), the dotted line with C and W denotes the center of a quasi-vesicle and the center of the wall in a quasi-vesicle, respectively. Note that (a), (b), and (c) have different scales.

length of the hydrophilic blocks. The conclusion that there is a polydispersity-driven segregation of copolymers can also be obtained from the density profiles of the hydrophobic blocks, as shown in Figure 3c. For the copolymers with shorter hydrophilic blocks, the hydrophobic blocks are localized in the center of the structure. On the other hand, for the copolymers with longer

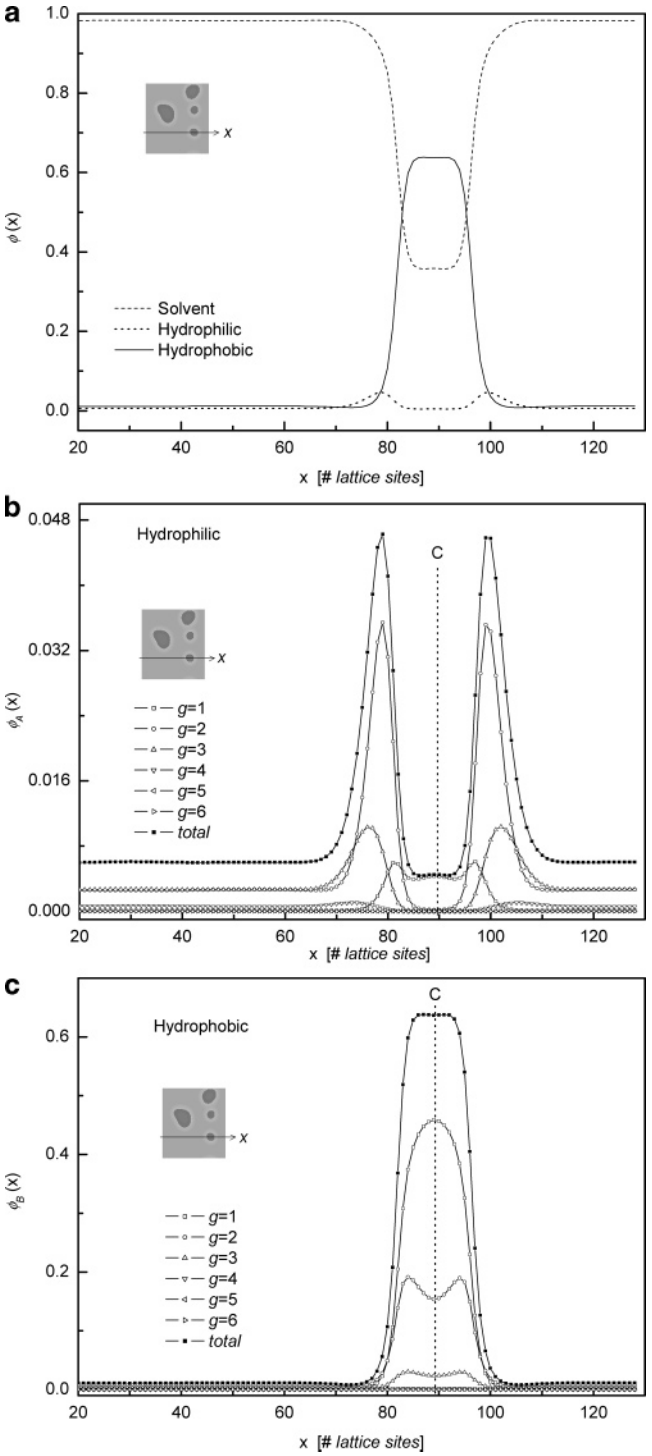

Figure 4. Density distribution of the micelle for polydisperse A (hydrophilic) blocks with $I_{pdi}^{A} = 3.5$ and $n_g = 6$. The inset shows two-dimensional density configurations corresponding to Figure 1d. (a) Density contributions from A (hydrophilic) segments, B (hydrophobic) segments, and S (solvent). (b, c) Contributions from each of the n_g terms. In (b) and (c), the dotted line with C denotes the center of a micelle. Note that (a), (b), and (c) have different scales.

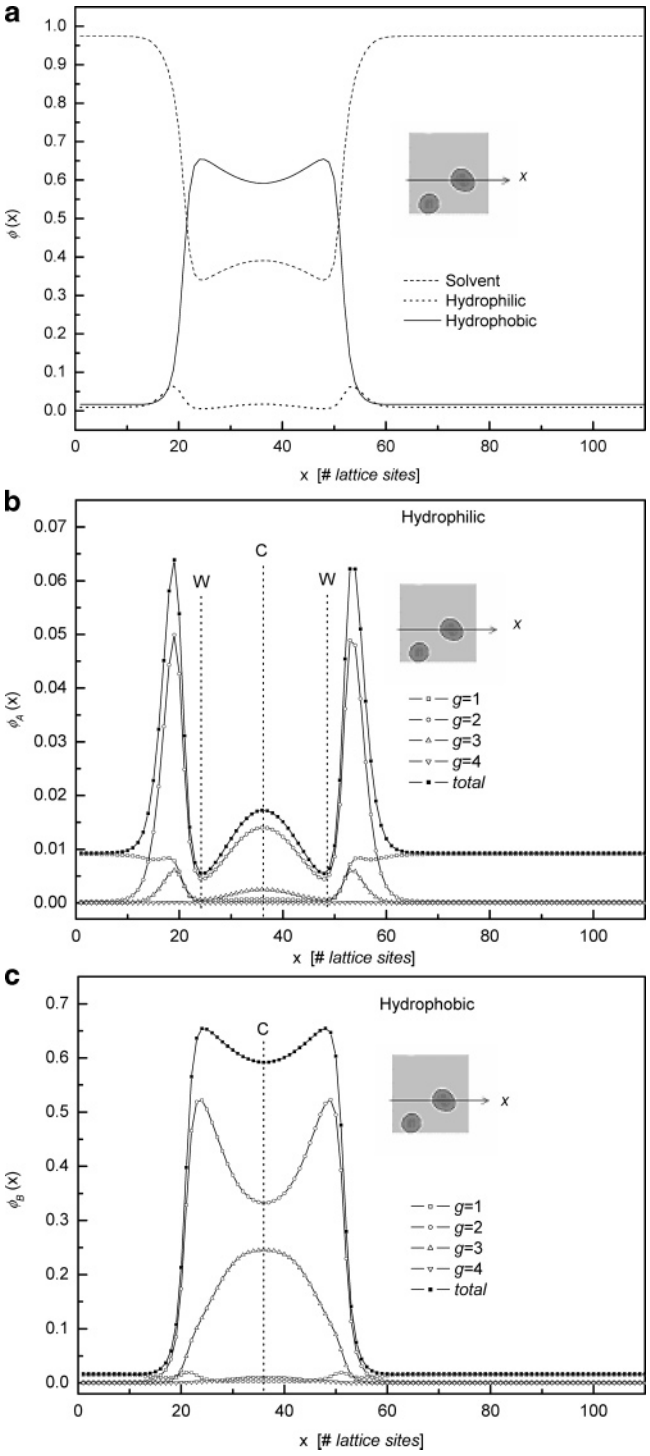

Figure 5. Density distribution of the quasi-vesicle for the polydisperse B (hydrophobic) blocks with $I_{pdi}^{B} = 1.667$ and $n_g = 4$. The inset shows two-dimensional density configurations which are obtained from initial density fluctuation β (equals to 10^{-6}) with the diblock parameters $\chi_{AB}N_n = 24.0$, $\chi_{BS}N_n = 30.0$, and $\chi_{AS}N_n = -9.0$. (a) Density contributions from A (hydrophilic) segments, B (hydrophobic) segments and S (solvent). (b, c) Contributions from each of the n_g terms. In (b) and (c), the dotted line with C and W denotes the center of a quasi-vesicle and the center of the wall in a quasi-vesicle, respectively. Note that (a), (b), and (c) have different scales.

hydrophilic blocks, the hydrophobic blocks are localized at the interior interface, forming a vesicle-like structure. From these observations we may argue that the conversion from vesicle to quasi-vesicle for large polydispersity index is driven by the localization of the shorter hydrophilic blocks into the interior of the structure. These theoretical predictions are in good agreement with available experimental observations. In particular, we would like to point out that, on the basis of their experimental observations, Eisenberg and co-workers have suggested that the shorter chains preferentially segregate to the inner surface of the wall, while the longer chains prefer the outside of the wall.[41]

When the polydispersity index is increased further, up to $I^{A}_{dpi} = 3.5$, a mixture of spherical micelles and quasi-vesicles is observed, as shown in Figure 1d. As indicated in Figure 4a, for the micelles, the density profiles are characterized by a unimodal feature.[26] From the density distributions of the different components (Figure 4b,c), the polydispersity-driven segregation is still present. In the corona region, the short hydrophilic blocks are localized at the interfaces while the longer blocks are extended. In the interior of the micelle, only a minor part of the longer hydrophilic blocks are present. These features are quite different from the quasi-vesicles.

3.2. Polydispersity on Hydrophobic Blocks. This subsection focuses on the case in which the hydrophobic block (B block) is polydisperse while the hydrophilic block (A block) is monodisperse. In the calculations n_g is chosen to be 4, which gives accurate results for our systems, as demonstrated above. Typical structures for this system are shown in Figure 5. In particular, the inset in Figure 5a shows the two-dimensional density distribution obtained with a polydispersity index $I^{B}_{pdi} = 1.667$. The density profiles of the different A, B, and solvent shown in Figure 5a indicate that this structure can be classified as a quasi-vesicle. In comparison with the quasi-vesicle in the case of polydisperse hydrophilic blocks, the polydispersity of the hydrophobic blocks leads to completely different characteristics. In the corona region, the A blocks with different B chain length show a very interesting density distribution. For shorter B blocks ($g = 1$), the A-blocks are distributed uniformly in the solvent, indicating that they are not associated with any particular micelles. This implies that the copolymers with shorter hydrophobic blocks behave like hydrophilic homopolymers. On the other hand, for longer B blocks ($g = 2, 3, 4$), the A blocks are localized at the surface of the structures. In the interior of the structure (Figure 5c), the shortest B blocks ($g = 1$) are distributed uniformly across the structure, with a slight localization at the A/B interface. The contribution from $g = 2$ shows a marked bimodal profile, indicating the formation of a quasi-vesicle structure. Finally, the longer B blocks ($g = 3, 4$) extend to the central domain of the quasi-vesicle. This behavior can be understood by noticing that the miscibility of the A/B blocks is determined by the relative chain lengths of the two blocks. Longer B blocks lead to a large miscibility of the A block in the interior of the structure. Similarly, shorter B blocks lead to a relatively large miscibility of the copolymers in the solvents, thus the delocalization of the $g = 1$ component. Larger B block polydispersity index, e.g. $I^{B}_{pdi} = 3.0$, leads to spherical micelles with unimodal density distribution for the hydrophobic blocks, similar to the case of polydisperse A blocks.

4. Conclusions

Using a 2D real-space self-consistent-field theory of polydisperse diblock copolymer solutions, the self-assemblies of vesicles and micelles are studied. The diblock copolymers are assumed to have a monodisperse block and a polydisperse block. Either the hydrophilic or the hydrophobic blocks can be polydisperse in the study. The molecular weight distribution is modeled using the Schulz distribution, which is a continuous chain length distribution amenable to analytic and numeric analysis. The study focuses on the effect of polydispersity on the structure of diblock copolymer vesicles in dilute solutions. For the case of polydisperse hydrophilic blocks, the simulation results show that larger polydispersity index I^{A}_{pdi} favors the formation of quasi-vesicles due to the segregation of the copolymers according to chain lengths. Two types of chain segregations are observed. First of all, it is observed that the shorter chains tend to localize at the A/B interfaces, while the longer chains extend to the outer surfaces. Second, and more interestingly, there is a separation of copolymers with different chain lengths to the inner and outer monolayers of the bilayer. The prediction about the copolymer segregation and the formation of quasi-vesicles is in good agreement with experimental results. For the case of polydisperse hydrophobic blocks, moreover, the simulation results show that larger I^{B}_{pdi} favors the formation of quasi-vesicles due to the segregation of the copolymers. In particular, the longer hydrophobic blocks dominate the center of the vesicle. In addition, the density distributions of the monodisperse hydrophobic (hydrophilic) blocks are affected by the polydisperse hydrophilic (hydrophobic) blocks.

Acknowledgment. The research is supported by the General Program (203074050, 90403022) and the Major Program (20490220) of National Natural Science Foundation of China (NSFC). A.C.S. acknowledges the support by the Natural Science and Engineering Research Council (NSERC) of Canada and the Research Corporation.

References and Notes

(1) Hadjichristidis, N.; Pispas, S.; Floudas, G. *Block Copolymers: Synthetic Strategies, Physical Properties, and Applications*; John Wiley & Sons: Hoboken, NJ, 2003.
(2) Gao, Z. S.; Eisenberg, A. *Macromolecules* **1996**, *26*, 7353.
(3) Zhang, L.; Eisenberg, A. *Science* **1995**, *268*, 1728.
(4) Yu, K.; Eisenberg, A. *Macromolecules* **1996**, *29*, 6359.
(5) Zhang, L.; Yu, K.; Eisenberg, A. *Science* **1996**, *272*, 1777.
(6) Zhang, L.; Eisenberg, A. *Macromolecules* **1996**, *29*, 8805.
(7) Luo, L.; Eisenberg, A. *Langmuir* **2001**, *17*, 6804.
(8) Choucair, A.; Lavigueur, C.; Eisenberg, A. *Langmuir* **2004**, *20*, 3894.
(9) Discher, D. E.; Eisenberg, A. *Science* **2002**, *297*, 967.
(10) Lipowsky, R. *Nature (London)* **1991**, *349*, 475.
(11) Jülicher, F.; Lipowsky, R. *Phys. Rev. Lett.* **1993**, *70*, 2964.
(12) Umeda, T.; Nakajima, H.; Hotani, H. *J. Phys. Soc. Jpn.* **1998**, *67*, 682.
(13) Noguchi, H.; Takasu, M. *Phys. Rev. E* **2001**, *64*, 041913.
(14) Noguchi, H.; Takasu, M. *J. Chem. Phys.* **2001**, *115*, 9547.
(15) Bernardes, A. T. *J. Phys. II* **1996**, *6*, 169.
(16) Bernardes, A. T. *Langmuir* **1996**, *12*, 5763.
(17) Yamamoto, S.; Maruyama, Y.; Hyodo, S.-A. *J. Chem. Phys.* **2002**, *116*, 5842.
(18) Edwards, S. F. *Proc. Phys. Soc.* **1965**, *85*, 613.
(19) Helfand, E. *J. Chem. Phys.* **1975**, *62*, 999. Helfand, E. *Macromolecules* **1975**, *8*, 552.
(20) Matsen, M. W.; Schick, M. *Phys. Rev. Lett.* **1994**, *72*, 2660.
(21) Noolandi, J.; Shi, A.-C.; Linse, P. *Macromolecules* **1996**, *29*, 5907.
(22) Drolet, F.; Fredrickson, G. H. *Phys. Rev. Lett.* **1999**, *83*, 4317. Drolet, F.; Fredrickson, G. H. *Macromolecules* **2001**, *34*, 5317.
(23) Maniadis, P.; Thompson, R. B.; Rasmussen, K. Ø.; Lookman, T. *Phys. Rev. E* **2004**, *69*, 031801. Thompson, R. B.; Rasmussen, K. Ø.; Lookman, T. *J. Chem. Phys.* **2004**, *120*, 3990.
(24) Fredrickson, G. H.; Ganesan, V.; Drolet, F. *Macromolecules* **2002**, *35*, 16.
(25) Bohbot-Raviv, Y.; Wang, Z.-G. *Phys. Rev. Lett.* **2000**, *85*, 3428.
(26) He, X. H.; Liang, H. J.; Huang, L.; Pan, C. Y. *J. Phys. Chem. B* **2004**, *108*, 1731.
(27) Doi, M.; Edwards, S. *The Theory of Polymer Dynamics*; Clarendon Press: Oxford, 1986.
(28) Teraoka, I. *Polymer Solutions*: *An Introduction to Physical Properties*; John Wiley & Sons: New York, 2002.
(29) Jian, T.; Anastasiadis, S. H.; Semenov, A. N.; Fytas, G. *Macromolecules* **1995**, *28*, 2439.

(30) Dobrynin, A. V. *Macromolecules* **1997**, *30*, 4756.
(31) Milner, S. T.; Witten, T. A.; Cates, M. E. *Macromolecules* **1989**, *22*, 853.
(32) Pagonabarraga, I.; Cates, M. E. *Europhys. Lett.* **2001**, *55*, 348.
(33) Matsen, M. W.; Bates, F. S. *Macromolecules* **1995**, *28*, 7298.
(34) Thompson, R. B.; Matsen, M. W. *Phys, Rev. Lett.* **2000**, *85*, 670.
(35) Fredrickson, G. H.; Sides, S. W. *Macromolecules* **2003**, *36*, 5415.
(36) Sides, S. W.; Fredrickson, G. H. *J. Chem. Phys.* **2004**, *121*, 4974.
(37) Schulz, G. V. Z. *Z. Phys. Chem. (Munich)* **1939**, *B43*, 25.
(38) Tzeremes, G.; Rasmussen, K. O.; Lookman, T.; Saxena, A. *Phys. Rev. E* **2002**, *65*, 041806.
(39) Sides, S. W.; Fredrickson, G. H. *Polymer* **2003**, *44*, 5859.
(40) Press, W. H.; Teukolsky, S. A.; Vetterling, W. T.; Flannery, B. P. *Numerical Recipes in C: The Art of Scientific Computing*, 2nd ed.; Cambridge University Press: Boston, 1992.
(41) Terreau, O.; Luo, L.; Eisenberg, A. *Langmuir* **2003**, *19*, 5601.

MA050424J